FISEVIER

### Contents lists available at ScienceDirect

# Scripta Materialia

journal homepage: www.elsevier.com/locate/scriptamat



# Material hardness at strain rates beyond $10^6$ s<sup>-1</sup> via high velocity microparticle impact indentation



Mostafa Hassani a,b,\*, David Veysset C, Keith A. Nelson C,d, Christopher A. Schuh a,\*

- <sup>a</sup> Department of Materials Science and Engineering, MIT, Cambridge, MA 02139, United States
- <sup>b</sup> Sibley School of Mechanical and Aerospace Engineering, Cornell University, Ithaca, NY 14853, United States
- <sup>c</sup> Institute for Soldier Nanotechnologies, MIT, Cambridge, MA 02139, United States
- <sup>d</sup> Department of Chemistry, MIT, Cambridge, MA 02139, United States

#### ARTICLE INFO

Article history:
Received 14 September 2019
Revised 15 October 2019
Accepted 22 October 2019
Available online 1 November 2019

Keywords: Hardness Impact Indentation High strain rate

#### ABSTRACT

Despite advances in mechanical testing at small scales and testing at high strain rates, studies of mechanical behavior of materials remain largely qualitative in the regimes where these two conditions overlap. Here, we present an approach based on microparticle impact indentation to determine material hardness at micron scales and at high strain rates. We employ laser ablation to impact ceramic alumina microparticles (as indenter) onto two model materials, namely copper and iron. We use real time measurements of impact and rebound velocities together with post-impact measurements of indentation volume to determine material hardness at strain rates beyond  $10^6 \ s^{-1}$ .

© 2019 Acta Materialia Inc. Published by Elsevier Ltd. All rights reserved.

The notion that contact impressions are related to mechanical properties of materials, particularly material strength or hardness, is the basis for a variety of impression and indentation tests developed over the last century. The advent of instrumented indentation, thanks to the development of new sensors and actuators, extended the concept to submicron scales [1]. Nanoindentation is now routinely used for measuring not only material hardness and stiffness but also other mechanical properties including hardening, fracture, and creep parameters [2-6]. Nanoindentation also enabled fundamental studies of materials phenomena including, for instance, defect nucleation, strain localization, and phase transformation [7]. With continuing miniaturization of many technological applications involving thin films and microelectronic devices [8,9], nanoindentation is now an indispensable approach for understanding mechanical behavior of materials at small scales-which often largely deviates from that at macroscales [10-14].

Mechanical response of materials can also dramatically change with strain rate [15]. As the deformation rate increases, phonon and electron viscosity [16] and/or relativistic effects [17] begin to govern dislocation response over thermal activation [18–20]. At high strain rates, mass inertia can lead to propagation of elastic, plastic, and shock waves whose interaction with microstructural features determines the morphological characteristics of de-

E-mail addresses: hassani@cornell.edu (M. Hassani), schuh@mit.edu (C.A. Schuh).

formation and failure [21]. What is more, at high strain rates, the thermal diffusion distance decreases with the deformation duration, leading to pronounced temperature inhomogeneities within the material [22,23]. Various experimental techniques such as Taylor impact tests [24], the Kolsky (Split-Hopkinson) bar [25], and gas gun impact experiments [26] have been developed to study phenomena emerging at high strain rates. Such experiments have provided invaluable insight into material response in a wide range of applications from crashworthiness to ballistic impacts, to machining, surface finishing, and recently additive manufacturing.

Fig. 1a depicts how indentation and high strain testing probe mechanical behavior in different regions of the characteristic sizevelocity map compared to the conventional macroscale mechanical testing; here the strain rate appears as a series of contours defined by the ratio of velocity and size. Indentation involves similar characteristic velocities compared to macroscale mechanical testing but focuses on small scales. High rate experiments remain largely at macroscales but extend the velocity axis. What remains largely unexplored in a quantitative sense is mechanical behavior of materials at small scales and high strain rates together. There have been interesting attempts to achieve both conditions together by extending high strain rate testing to smaller scales, e.g., miniaturized Kolsky bar experiments [27,28] or by increasing velocity in the indentation experiments using a pendulum [29,30], gravity and gas guns [31], or incident bars [32] to impact the indenter tip on the test substrate in so-called dynamic indentation testing.

<sup>\*</sup> Corresponding authors.

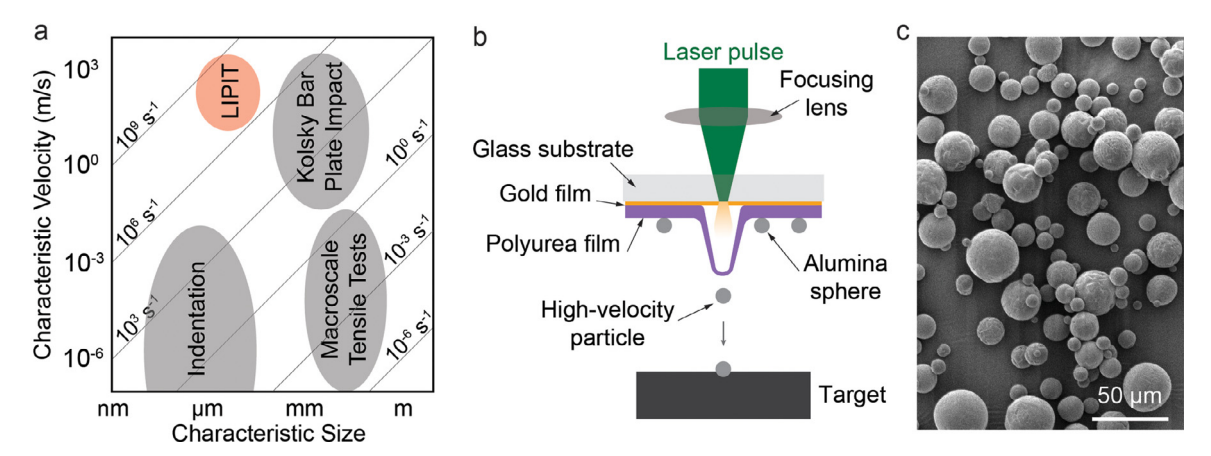


Fig. 1. (a) Different mechanical testing approaches in the characteristic size-velocity space; the contours show the ratio of these parameters, i.e., the strain rate. (b) Experimental platform for laser-induced microparticle impact test and real-time imaging. (c) Scanning electron micrograph of alumina powder particles from which individual  $\sim$ 10–19 µm particles were selected for use as indenters.

Nevertheless, strain rates beyond  $10^6 \text{ s}^{-1}$  remain largely quantitatively unexplored.

One can achieve strain rates beyond  $10^6 \text{ s}^{-1}$  by a simultaneous decrease in length scale and increase in velocity, e.g., by high velocity impact of micrometer-sized particles [33-41]. This is an interesting regime where micrometer-level length scales of material are involved with an unusually intense deposition of high energy during nanosecond-level time scales. In this letter we measure material hardness in this regime, as depicted in Fig. 1b, using laser induced microparticle impact tests (LIPIT). In our experiments, we launch spherical microparticles of alumina (See Fig. 1c) to impact two model materials, namely pure copper and pure iron. We measure the amount of plastic work dissipated into the material by direct measurements of impact and rebound velocities of the particles. We also measure indentation volumes through post-impact observations. The two parameters together enable quantification of material hardness at the strain rates experienced during the microparticle impacts, i.e., beyond  $10^6$  s<sup>-1</sup>.

Shown in Fig. 1b is a schematic of an all-optical microballistic platform [35-39] that we used for the laser-induced particle impact experiments. The launch pad in our setup consisted of a 210-µm thick glass substrate (bottom layer), a 60-nm thick gold layer (intermediate layer), and a 30-µm thick polyurea film (top layer). Particles to be launched are dispersed on top of the launching pad. We focus a laser pulse (pulsed Nd:YAG, 10-ns duration, 532-nm wavelength, pulse energy up to 60 mJ) into a 50-µm diameter spot size on the gold film whose ablation drives the polyurea film forward and accelerates a particle of alumina toward the target material. Different velocities can be achieved by adjusting the laser energy (from 2 to 60 mJ). The distance between the launching pad and the target is typically 1 mm. We capture the particle approach, impact on the target material, and its rebound in real time using a µs laser pulse (10-µs duration, 640-nm wavelength) for illumination and a high-speed camera (SIMX 16, Specialised Imaging). The impacts are normal to the surface of the target within a cone of  $\pm$  3°. Impact velocities are measured with an uncertainty of  $\pm 2\%$ . We have conducted all impact experiments in a site-specific fashion so that we could analyze all impact-induced indentations post-mortem and associate indentation volume with the deposited energy per impact. Post-mortem observations of the indentations and surface profilometry were performed with a Tescan Mira3 high-resolution scanning electron microscope (SEM) and a 3D laser scanning confocal microscope, VK-X200 series, Keyence.

Alumina powder particles with nominal particle sizes of  $20\,\mu m$  were purchased from Inframat Advanced Materials LLC (Amherst, USA). Prior to each impact, we measured the diameter of the par-

ticle to be launched using a secondary CCD camera. A copper plate with 3.175 mm thickness and an iron rod with 12 mm diameter were purchased from Alfa Aesar (Ward Hill, USA) and OnlineMetals (Seattle, USA) respectively. A diamond blade on a precision cutter was used to extract  $12\times12$  mm plates for use as the target materials for the impact experiments. The target surfaces were ground and polished to nominally  $0.04\mu m$  mirror finish prior to the impact experiments.

Fig. 2a and b shows two exemplar snapshots of the impact experiment where two spherical alumina particles traverse downward from the top of the field of view and impact a copper substrate (Fig. 2a) and an iron substrate (Fig. 2b) at the bottom. The particle impacting copper is  $14.0 \,\mu m \ (\pm \ 0.5 \,\mu m)$  in diameter and the one impacting iron is  $14.2 \,\mu\text{m}$  ( $\pm 0.5 \,\mu\text{m}$ ). The impact on copper occurs at  $425 \,\mathrm{m/s}~(\pm~8\,\mathrm{m/s})$  velocity whereas the impact on iron occurs at  $657 \,\mathrm{m/s}~(\pm~13\,\mathrm{m/s})$ . Both particles rebound with a fraction of their inbound velocity, 9.5% for the impact on copper and 11.5% for the impact on iron. About 99% of the kinetic energy of these particles is therefore dissipated upon impact, which results in the formation of the indentations shown in the SEM micrographs of Fig. 2c for copper and Fig. 2d for iron. These impression sites are consistent with a spherical indentation geometry, although there are slight irregularities or inhomogeneities, probably due to anisotropic/inhomogeneous plasticity in the substrate, or possibly mild shape distortions in the incident particles.

We do not observe indications of plastic deformation in the rebounding alumina particles, e.g., significant deviation from sphericity, in our real time observations, nor do we observe fracture, melting, or erosion of the substrate materials in our SEM micrographs. Therefore, we proceed confident in the assumption that plastic deformation of the substrate is the far dominant operative mechanism that dissipated the energy of the incoming particles. Of course, plasticity redistributes the dissipating energy through a combination of microstructural evolution and heat generation. Here, we keep the assumption typical in nanoindentation studies that the results are not significantly affected by friction between indenter and substrate [42–44], but highlight that friction effects have been found significant in other high velocity impact situations [45], so this is a topic worthy of future exploration.

Fig. 2e and f are topological reconstructions of the same indentations shown in Fig. 2c and d using laser confocal microscopy, and Fig. 2g shows a cross-sectional line scan across a diameter, comparing the two indentation profiles. In order to satisfy volume conservation in plasticity, the base surface in our analysis is set such that the pile-up volume conserves the indentation volume. The contours show the height deviations of the post-impact

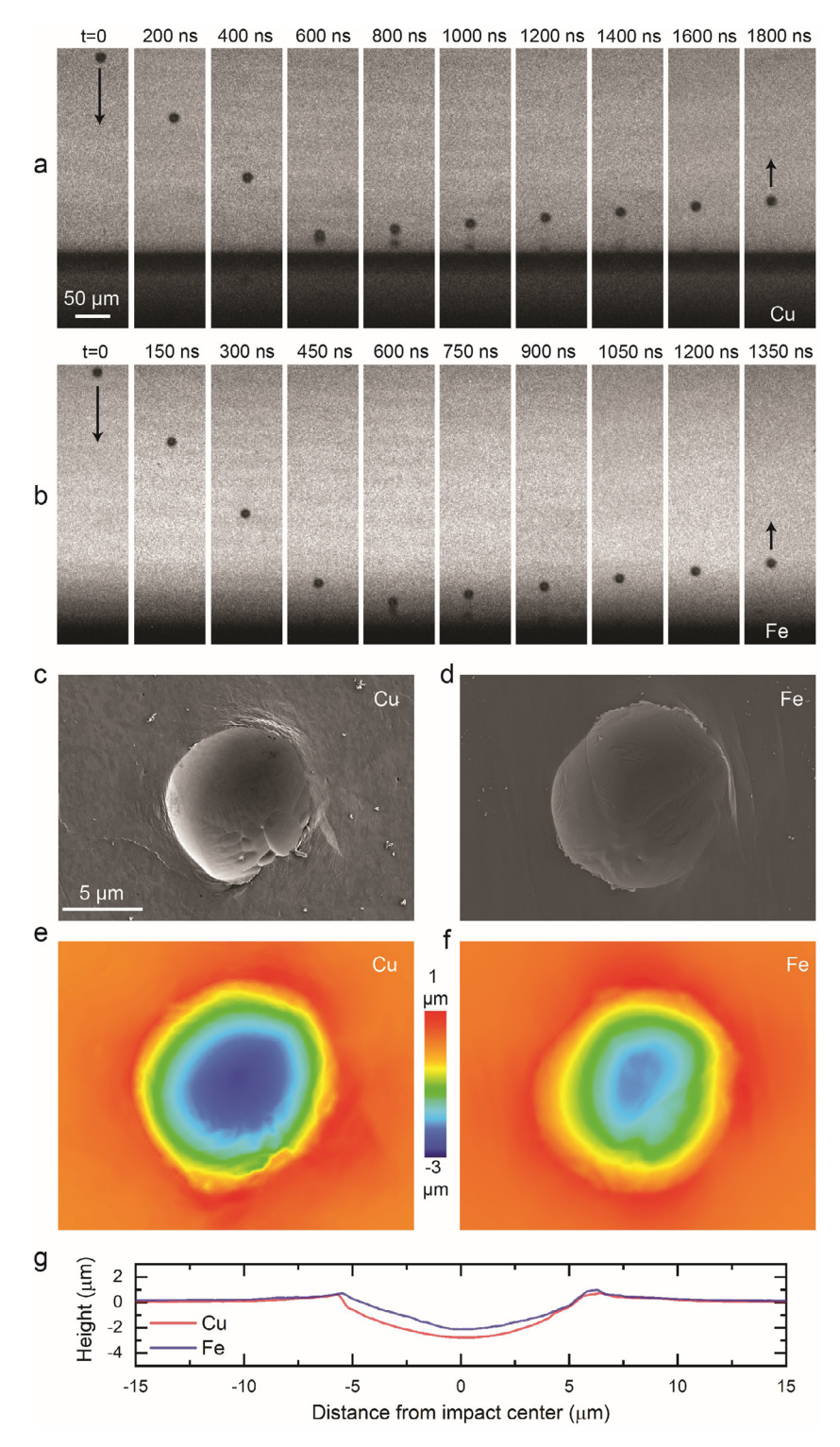
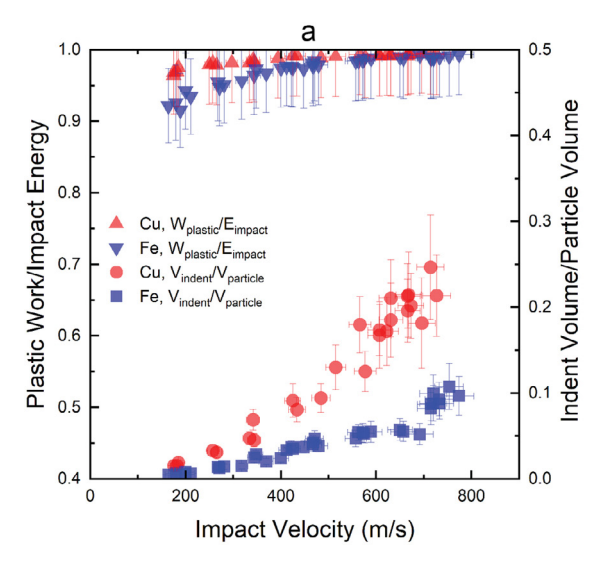


Fig. 2. (a,b) Multi-frame sequences with 5 ns exposure times showing (a) 14.0-µm- and (b) 14.2-µm-alumina particles arriving from the top of the field of view and impacting (a) a copper substrate at 425 m/s and (b) an iron substrate at 657 m/s. (c,d) Scanning electron micrographs of the (c) copper and (d) iron impact-induced indentations. (e,f) Laser confocal images of (e) the copper and (f) the iron indentations. (g) a 1-D surface profile of the copper and iron indentations.

deformed surface from the pre-impact flat surface. We measured a maximum penetration of  $2.79\,\mu m$  for copper and  $2.13\,\mu m$  for iron. The indentation volumes are 131 and 91  $\mu m^3$  for copper and iron respectively. It is interesting to note that while the impact velocity is higher in the case of iron (more energy is dissipated into iron compared to copper), the iron indentation is shallower and smaller in volume than the copper one. This stems from the fact that iron is harder than copper and foreshadows the use

of such data from microparticle impact experiments to determine hardness.

Greater insight is provided by Fig. 3a where we plot the ratio of the energy consumed for the plastic deformation of the target material, hereinafter called plastic work, to the total impact energy in a wide range of impact velocity, from 164 to 774 m/s. We calculate the ratio by measuring both impact and rebound velocities from the real time observations according to the following



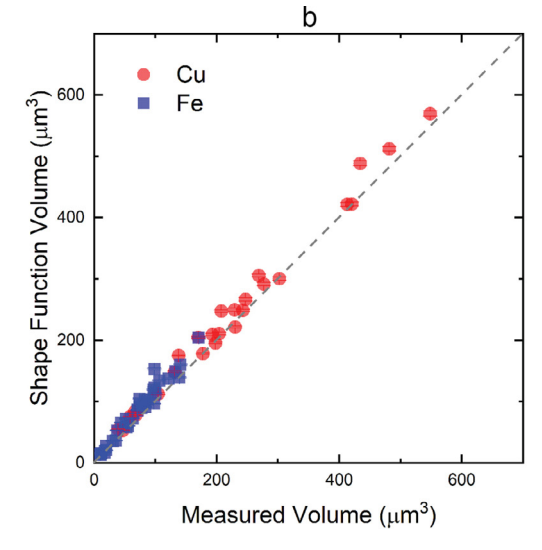


Fig. 3. (a) Variation of the ratio between the impact-induced plastic work and the total impact energy (left axis) and the ratio between the indentation volume and the particle volume (right axis) with impact velocity. (b) Comparison of the shape function-based estimation of the indentation volume with the direct measurement shows a reasonable match.

equation:

$$\frac{W_{plastic}}{E_{impact}} = 1 - \left(\frac{v_r}{v_i}\right)^2 \tag{1}$$

where  $W_{Plastic}$  is the plastic work,  $E_{impact}$  is the impact energy,  $v_i$  is the impact velocity and  $v_r$  is the rebound velocity. We observe that a considerable fraction of the impact energy is dissipated as the plastic work in our experiments. The fraction is greater than 90% even at the lowest impact velocity and it approaches 100% as impact velocity increases. The plastic work done on copper is greater than the plastic work done on iron only by a few percent at the lower impact velocities with the difference becoming negligible at the higher impact velocities.

Superimposed on the same plot of Fig. 3a is the variation of the ratio of the indentation volume to the impacting particle volume. We have calculated the former by laser confocal analysis of the indentations and the latter by measuring the diameter of the particles before launch. We observe that indentation volume increases with impact velocity with an ascending slope. At the same impact velocity, while the plastic work done on iron is close to the plastic work done on copper, the indentation volume in copper is larger than that in iron by a factor of 2–3. This observation, in principle, means at the strain rates of these impact experiments, iron demonstrates a resistance to plastic deformation that is 2–3 times higher than copper.

To determine the absolute values of hardness, we turn to the definition of dynamic hardness as being the ratio of the plastic work to the indentation volume:

$$Hardness = \frac{W_{plastic}}{V_{indentation}} = \frac{(1/2) \times m_p \times (v_i^2 - v_r^2)}{V_{indentation}}$$
(2)

where  $m_p$  is the mass of the impacting particle,  $V_{indentation}$  is the indentation volume and  $v_i$  and  $v_r$  are the impact and rebound velocities. Having measured the impact and rebound velocities, one can directly measure the indentation volume using post-impact surface topography measurements—as we did here via confocal laser microscopy—to calculate the hardness. Alternatively, one can estimate the indentation volume based on the measurements of its width or depth and considering a spherical shape function for the indenter, as typically done in nanoindentation testing. Once either indentation depth, h, or width, 2a, are known, the other can be calculated using  $(d_p-h)\times h=a^2$  with  $d_p$  being the particle diameter. The indentation volume can then be calculated using

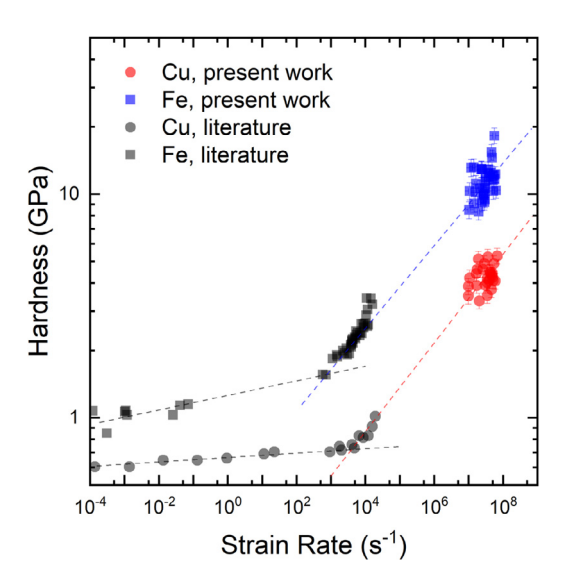


**Fig. 4.** Variation of hardness for copper and iron over twelve decades of strain rates. For the sake of comparison, we have taken the data for the lower strain rate regimes from the measurements of material strength in refs. [40,41]. To convert the strength data from literature to hardness we have used a factor of 3. The dashed lines are a guide to the eye.

 $V_{indentation} = \frac{1}{6}\pi h \times (3a^2 + h^2)$ . In Fig. 3b we compare such shape function-based estimation of the indentation volumes with the directly measured ones, which produces a reasonable match. Therefore, we propose that alternate forms of Eq. (2) can be credibly used to calculate the hardness particularly when the direct measurement of the indentation volume is not in hand, such as:

$$\textit{Hardness} = \frac{\rho_p \times d_p^3 \times \left(\nu_i^2 - \nu_r^2\right)}{2 \times h^2 \times (3d_p - 2h)} \tag{3}$$

where  $\rho_p$  is the density of the particle.

In this work we have calculated the hardness for all impact experiments using our direct measurements of the indentation volume and Eq. (2). We associate with every impact a characteristic strain rate using  $\dot{\varepsilon} = v_i/d_p$  where  $d_p$  is the diameter of the impacting particle. Fig. 4 shows the variation of hardness with strain rate. Here, the data for  $\sim 10^6-10^7~{\rm s}^{-1}$  regime is provided by the present

impact experiments and the data for the lower strain rates regimes are taken from uniaxial data in refs. [46,47], converted with a Tabor factor of 3 to a hardness value; error from this assumed conversion is negligible on the scales of the trends in Fig. 4.

Together, the two sets of data in Fig. 4 show how material hardness changes over twelve decades of strain rate. The data from literature show that (i) iron is harder than copper, (ii) hardness increases with strain rate, and (iii) the strain rate sensitivity of hardness apparently increases beyond  $10^3-10^4$  s<sup>-1</sup>. This latter is due to the change of deformation mechanism from thermally activated dislocation motion to dislocation drag [46]. With our impact experiments, we also measure higher hardness for iron compared to copper, observe an overall increasing hardness with strain rate and note a trend that is in line with the extrapolation of the literature data beyond  $10^3-10^4$  s<sup>-1</sup>. Fig. 4 demonstrates that real time observations in microparticle impact tests when further augmented with the post-impact analysis of the indentations can be a reliable approach to characterize material hardness at high strain rates. Although high strain rate testing of mechanical behavior of materials beyond  $10^6 \text{ s}^{-1}$  have been conducted using shocks [48,49] or explosives [50,51], which are often targeted to measure spall strength, to the best of our knowledge, the present work is a first-of-its-kind indentation approach to measure material strength or hardness at such high strain rates.

To summarize, with a concurrent decrease in length scale to the micron scale and increase in velocity to hundreds of m/s, we have proposed an indentation-based approach that enables measurement of material hardness at strain rates beyond 10<sup>6</sup> s<sup>-1</sup>. We have shown that impact of rigid spherical microparticles onto deformable materials and their rebounds, if captured in real time, can be used to measure plastic work done to make the indentations. The amount of plastic work together with the indentation volume then can be used to measure material hardness. We have demonstrated the concept for alumina spherical particles as rigid indenters and two pure metals—copper and iron—as substrate materials. Our approach, however, has no limitations for extension to other indenter/substrate material pairs and should prove useful for studies of material hardness and strain rate sensitivity at high strain rates.

# **Declaration of Competing Interest**

The authors declare that they have no known competing financial interests or personal relationships that could have appeared to influence the work reported in this paper.

## Acknowledgment

This work was primarily supported at MIT by the U.S. Department of Energy, Office of Science, Office of Basic Energy Sciences, Division of Materials Sciences and Engineering under Award DE-SC0018091. MH's work at Cornell was supported through a cooperative research agreement with the U. S. Army Research Laboratory, Contract: W911NF-15-2-0034, and the Cornell Center for Materials Research Shared Facilities which supported through the NSF MR-SEC program (DMR-1719875).

#### References

- [1] W.C. Oliver, G.M. Pharr, J. Mater. Res. 7 (1992) 1564-1583.
- [2] G.M. Pharr, W.C. Oliver, MRS Bull. 17 (1992) 28-33.
- [3] X. Li, B. Bhushan, Mater. Charact. 48 (2002) 11-36.
- [4] R. Saha, W.D. Nix, Acta Mater. 50 (2002) 23-38.
- [5] C.A. Schuh, T.G. Nieh, Acta Mater, 51 (2003) 87–99
- [6] J.M. Wheeler, D.E.J. Armstrong, W. Heinz, R. Schwaiger, Curr. Opin. Solid State Mater. Sci. 19 (2015) 354-366.
- [7] C.A. Schuh, Mater. Today 9 (2006) 32-40.
- [8] A.R. Krauss, O. Auciello, D.M. Gruen, A. Jayatissa, A. Sumant, J. Tucek, D.C. Mancini, N. Moldovan, A. Erdemir, D. Ersoy, M.N. Gardos, H.G. Busmann, E.M. Meyer, M.Q. Ding, Diam. Relat. Mater. 10 (2001) 1952-1961.
- [9] B. Bhushan, Microelectron. Eng. 84 (2007) 387-412.
- [10] A. Acharya, A. Roy, J. Mech. Phys. Solids 54 (2006) 1687–1710.
  [11] Y. Wang, M. Chen, F. Zhou, E. Ma, Nature 419 (2002) 912–915.
- [12] M.D. Uchic, D.M. Dimiduk, J.N. Florando, W.D. Nix, Science 305 (2004) 986-989.
- [13] J.R. Greer, W.C. Oliver, W.D. Nix, Acta Mater. 53 (2005) 1821-1830.
- [14] O.T. Abad, J.M. Wheeler, J. Michler, A.S. Schneider, E. Arzt, Acta Mater. 103 (2016) 483-494
- [15] M.A. Meyers, R.W. Armstrong, H.O.K. Kirchner, Mechanics and Materials: Fun-
- damentals and Linkages, Wiley, 1999. [16] R.W. Armstrong, W. Arnold, F.J. Zerilli, J. Appl. Phys. (2009) 105.
- [17] V. Nosenko, S. Zhdanov, G. Morfill, Phys. Rev. Lett. 99 (2007) 025002.
- [18] Y.N. Osetsky, D.J. Bacon, A. Serra, Philos. Mag. Lett. 79 (1999) 273-282.
- [19] J.W. Morris Jr., D.H. Klahn, J. Appl. Phys. 45 (1974) 2027–2038.
- [20] J.W. Morris Jr., D.H. Klahn, J. Appl. Phys. 44 (1973) 4882-4890.
- [21] J.M. Walsh, R.H. Christian, Phys. Rev. 97 (1955) 1544-1556.
- [22] M.A. Meyers, Y.B. Xu, Q. Xue, M.T. Pérez-Prado, T.R. McNelley, Acta Mater. 51 (2003) 1307-1325
- [23] H.A. Grebe, H.-R. Pak, M.A. Meyers, Metall. Trans. A 16 (1985) 761-775.
- [24] B. Plunkett, O. Cazacu, R.A. Lebensohn, F. Barlat, Int. J. Plast. 23 (2007) 1001-1021.
- [25] T. Nicholas, Exp. Mech. 21 (1981) 177-185.
- [26] G.R. Fowles, G.E. Duvall, J. Asay, P. Bellamy, F. Feistmann, D. Grady, T. Michaels, R. Mitchell, Rev. Sci. Instrum. 41 (1970) 984-996.
- [27] D. Jia, K.T. Ramesh, Exp. Mech. 44 (2004) 445-454.
- [28] J. Lim, W.W. Chen, J.Q. Zheng, Polym. Test. 29 (2010) 701-705
- [29] J.M. Wheeler, J. Dean, T.W. Clyne, Extrem. Mech. Lett. 26 (2019) 35-39.
- [30] J.R. Trelewicz, C.A. Schuh, Appl. Phys. Lett. 93 (2008) 171916.
- [31] A.S.M.I.H. Committee, ASM Handbook: Mechanical Testing and Evaluation, ASM International, 2000.
- [32] G. Subhash, B.J. Koeppel, A. Chandra, J. Eng. Mater. Technol. 121 (1999) 257-263.
- [33] J.-H. Lee, D. Veysset, J.P. Singer, M. Retsch, G. Saini, T. Pezeril, K.A. Nelson, E.L. Thomas, Nat. Commun. 3 (2012) 1164.
- [34] J.-H. Lee, P.E. Loya, J. Lou, E.L. Thomas, Science 346 (2014) 1092-1096.
- [35] D. Veysset, A.J. Hsieh, S. Kooi, A.A. Maznev, K.A. Masser, K.A. Nelson, Sci. Rep. 6 (2016) 2557
- [36] M. Hassani-Gangaraj, D. Veysset, K.A. Nelson, C.A. Schuh, Preprint at arXiv: 1612.08081 (2016).
- [37] D. Veysset, A.J. Hsieh, S.E. Kooi, K.A. Nelson, Polymer (Guildf) 123 (2017)
- [38] M. Hassani-Gangaraj, D. Veysset, K.A. Nelson, C.A. Schuh, Scr. Mater. 145 (2018)
- [39] M. Hassani-Gangaraj, D. Veysset, K.A. Nelson, C.A. Schuh, Phys. Rev. Lett. 119 (2017) 175701.
- [40] M. Hassani-Gangaraj, D. Veysset, K.A. Nelson, C.A. Schuh, Nat. Commun. 9 (2018) 5077.
- [41] M. Hassani-Gangaraj, D. Veysset, K.A. Nelson, C.A. Schuh, Appl. Surf. Sci. 476 (2019) 528-532.
- [42] H. Lee, J. Haeng Lee, G.M. Pharr, J. Mech. Phys. Solids 53 (2005) 2037-2069.
- [43] S. Kucharski, Z. Mróz, Mater. Sci. Eng. A 318 (2001) 65-76.
- [44] S. Suresh, A.E. Giannakopoulos, Acta Mater. 46 (1998) 5755-5767.
- E.J. Haney, G. Subhash, Exp. Mech. 53 (2013) 31-46.
- [46] R.W. Armstrong, S.M. Walley, Int. Mater. Rev. 53 (2008) 105-128.
- [47] D. Rittel, G. Ravichandran, A. Venkert, Mater. Sci. Eng. A 432 (2006) 191–201.
- [48] V.E. Fortov, V.V. K.ostin, S. Eliezer, J. Appl. Phys. 70 (1991) 4524-4531.
- [49] H. Tamura, T. Kohama, K. Kondo, M. Yoshida, J. Appl. Phys. 89 (2001) 3520-3522.
- [50] V. Livescu, J.F. Bingert, T.A. Mason, Mater. Sci. Eng. A 556 (2012) 155-163.
- [51] A.M. Karo, J.R. Hardy, F.E. Walker, Acta Astronaut. 5 (1978) 1041-1050.